

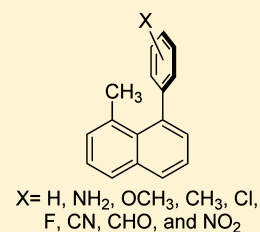
Influence of Substituents on the Through-Space Shielding of Aromatic Rings

Colin W. Anson[†] and Dasan M. Thamattoor^{*}

Department of Chemistry, Colby College, Waterville, Maine 04901, United States

S Supporting Information

ABSTRACT: A series of naphthalene derivatives, bearing a methyl group and a substituted phenyl ring in a 1,8-relationship, have been synthesized. The chemical shifts of the protons of the methyl group, which are pointed toward the shielding zone of the phenyl ring, were monitored as the phenyl substituents were varied. This work indicates that the shielding effect of the phenyl ring is not so severely altered by the substituents as to significantly influence the chemical shift of the methyl group. Nonetheless, within the small changes observed experimentally, there appears to be a tendency for electron-withdrawing X to shift the methyl signal downfield, whereas electron-donating X-groups cause a more upfield shift. Polarization and field effects are discussed as possible causes for this phenomenon. Chemical shifts computed for selected members of the series, using the recently published procedures of Rablen and Bally, are in agreement with the experimentally observed trends.



INTRODUCTION

In the 1930s, well before the advent of NMR spectroscopy, Pauling,¹ Lonsdale,² and London³ provided a ring current model to describe the diamagnetic anisotropy of benzene. Some 20 years later, Pople developed a magnetic dipole description of that model to explain the abnormal ¹H NMR chemical shift of benzene and other aromatic molecules.⁴ Since then, a variety of computational methods have been employed to analyze the relationships among ring currents, aromaticity, and NMR chemical shifts.⁵ The gist of these analyses, in a general sense, is that the circulation of π -electrons in aromatic rings, induced by an external magnetic field, deshields the outer protons, whereas the inner protons, or those located above/below the plane of the rings, are shielded. The ring current model for benzene has been vigorously challenged⁶ and defended.⁷ It has been also pointed out that the magnetic susceptibilities and shielding induced by the circulating π -electrons have a much larger component normal to the plane of the ring, and local effects, rather than the ring current, are more important determinants of the chemical shifts of peripheral protons.⁸ Indeed, the chemical shifts of phenyl protons are dramatically influenced by the presence of substituents due to various local factors such as inductive, field, and resonance effects.⁹ This can be seen, for example, in the large differences in chemical shifts of the ring protons in nitrobenzene (**1**) and aniline (**2**) compared to benzene (Figure 1).¹⁰ In the electron deficient aromatic ring of **1**, the proton signals are more downfield, and just the opposite is true for the electron-rich ring in **2**. The effects are particularly amplified at the ortho/para positions, and resonance contributions to electron densities have been invoked to explain these observations.^{9a}

But how do phenyl substituents affect the chemical shifts of protons in the *shielding zone* of the ring? Unfortunately, research literature addressing this question is surprisingly scant. To the best of our knowledge, there is just one computational report, that of Martin and co-workers, that specifically investigated the perturbation of diamagnetic anisotropy of

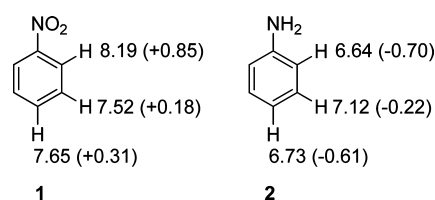


Figure 1. The chemical shifts (in δ ppm) of nitrobenzene and aniline ring protons. The difference from the shift of benzene protons (δ 7.34 ppm) are noted in parentheses. All shifts were measured in CDCl₃.¹⁰

aromatic rings by substituents, and the consequent effects on the shielding surface.¹¹ Using methane held at various positions above the plane of the phenyl ring in **1** and **2** (Figure 2),

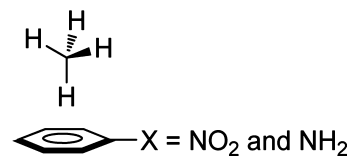


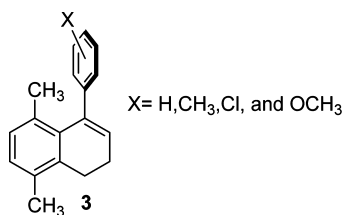
Figure 2. Martin's model for computing through-space shielding effects of the aryl ring in **1** and **2**.¹¹

Martin's group calculated the through-space shielding influence of the phenyl ring in these compounds and developed an algorithm to predict shielding above substituted aromatic rings. Their calculations suggest that "the perturbation due to the presence of a substituent has a relatively minor effect on the shielding surface and that the major effect is due to the aromatic ring." This result is in sharp contrast to the dramatic effect that these substituents have on the (de)shielding of the ring protons (*vide supra*).

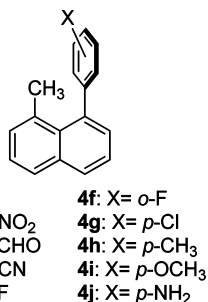
Received: October 25, 2011

Published: January 18, 2012

The literature on experimental work to test the through-space shielding effects of substituted phenyl rings is also limited to a solitary report, that of Penn and Mallory, in 1975.¹² Using a low field NMR spectrometer operating at 60 MHz and 3 as their model system, these workers attempted to find a correlation between the out-of-plane shielding of the phenyl ring and its substituent X. In this study, however, X was confined to just three substituents (besides hydrogen), with a narrow range of electronic properties. Common electron-withdrawing groups such as nitro, carbonyl, and cyano groups were conspicuously absent. Nonetheless, within this limited range of variously substituted 3, they noted that the chemical shifts of the methyl group projected toward the shielding zone of phenyl ring were ever so slightly upfield when X = OCH₃, Cl, and CH₃ compared to when X = H, but the variations among these chemical shifts were quite small. After considering several factors that could potentially influence shielding, such as substituent effects on ring currents and electric field effects of substituent polarities, Penn and Mallory concluded that “we do not think any sound inferences can be drawn from our data regarding the extent to which substituents influence ring currents.” While acknowledging that they could not provide a “fully satisfactory explanation” of their results, they offered the tentative suggestion that perhaps the anisotropy of the local magnetic susceptibilities of the substituents played an important role in determining shielding. They do note, however, that there is no conclusive evidence supporting such a hypothesis in their data.



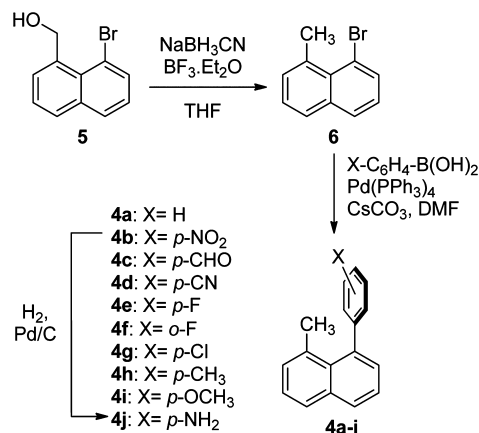
In this report, we describe a comprehensive study that builds on and extends the work of Penn and Mallory. We have prepared a series of 10 naphthalene derivatives (4a–j), related to 3, bearing a methyl group and a substituted phenyl ring in 1,8-relationship. This study includes a wide variety of substituents ranging from powerful electron-withdrawing groups to strong electron donors. The chemical shifts of the protons of the methyl group on the naphthalene ring, which are pointed toward the shielding zone of the phenyl ring, were monitored as the substituent X was varied.



RESULTS AND DISCUSSION

Syntheses of 4a–j. The syntheses of compounds 4a–j were accomplished according to the reactions shown in Scheme 1.

Scheme 1. Syntheses of Naphthalene Derivatives 4a–j



In the first step, commercially available (8-bromonaphthalen-1-yl) methanol (5) was reduced to 1-bromo-8-methylnaphthalene (6) following the procedure of Kesharwani and Larock.¹³ Subsequently, 4a–i were prepared by the palladium catalyzed Suzuki–Miyaura coupling of 6 with the appropriate aryl boronic acids.¹⁴ Catalytic reduction of 4b (X = NO₂) afforded 4j (X = NH₂), the tenth member of the series.

X-ray Crystallographic Studies. To obtain more structural information about our system, particularly the relative disposition of the methyl group and the substituted phenyl ring, we carried out single crystal X-ray diffraction experiments. We were able to grow suitable crystals for 7 of our 10 derivatives, namely, 4b–e and 4g–i, and solve their structures. These structures are shown in Figure 3, and selected data are summarized in Table 1. In each case, the crystal structure indicated that the phenyl ring was roughly orthogonal to the naphthyl ring but somewhat splayed away from the methyl group that is across from it. Two of the protons on the methyl group were oriented toward the shielding zone of the phenyl ring in the solid state. The distances of these protons from the centroid of the phenyl ring are collected in Table 1. Furthermore, the bond connecting the phenyl and naphthyl rings is the length of a normal single bond between two sp²-hybridized carbon atoms, indicating no conjugation between the two ring systems. These bond lengths, for example, are comparable to 1,8-diarylnaphthalenes where rotation of the phenyl ring is severely restricted.¹⁵ Thus, it appears unlikely that the electronic effects of the substituents on the phenyl ring are mesomerically transmitted into the naphthyl ring and influence the chemical shift of the methyl signal by altering local contributions.

¹H NMR Spectroscopy. All ¹H NMR spectra were recorded in deuterated chloroform at 500 MHz. The methyl signal of 1-methylnaphthalene appears at δ 2.685 ppm, and the installation of a phenyl ring at the 8-position, as in 4a, causes an upfield shift of the 1-methyl protons to δ 2.009 ppm (Table 2). Thus, it is clear that the phenyl ring exerts a substantial shielding influence, to the extent of δ 0.676 ppm (or 338 Hz), on the chemical shift of the methyl protons across from it. Table 2 also includes the chemical shifts of the methyl group on the naphthalene ring for the other derivatives employed in this study. Columns three and four in Table 2 show the difference in this chemical shift between each of the derivatives 4b–j and 4a and the ratio of this difference to the shielding exerted by the phenyl ring in 4a (i.e., 338 Hz), respectively. Thus, these last two columns provide a measure of how the various substituents X affect the shielding exerted by the phenyl ring.

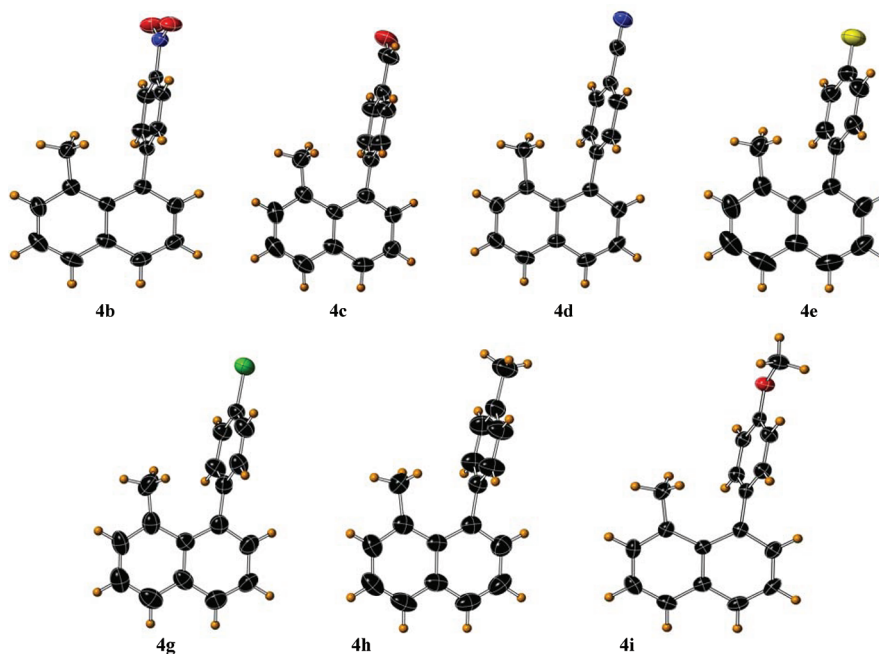


Figure 3. Single-crystal X-ray structures of 4b–e (top) and 4g–i (bottom).

As can be seen from Table 2, the substitution of X, spanning a broad range of electronic properties, into the phenyl ring in 4a, has but a very small effect on the chemical shift of the methyl group on the naphthalene ring. Of all the para substituents, the powerful electron-donating amino group exerts the strongest influence by inducing an 11% shift in the methyl signal toward the downfield direction as compared to the phenyl group itself (4j vs 4a). A similar downfield shift, albeit to a much smaller extent, is also observed for analogues containing other electron donors in the para position such as the methoxy (4i) and methyl (4h) groups. Although smaller, electron-withdrawing groups seem to have just the opposite effect on the chemical shift of the methyl signal, which is shifted ever so slightly more upfield; the *p*-cyano derivative (4d) induces the largest change followed by the *p*-nitro (4b) and *p*-formyl (4c) analogues. The effect of halogens on the chemical shifts is also interesting. Fluorine is an effective π donor but, by virtue of its high electronegativity, has a strong electron-withdrawing inductive effect. According to our data, placing fluorine in the para position, as in 4e, induces a slight upfield shift in the methyl signal that is similar to that of the *p*-nitro derivative (4b). Switching fluorine to the ortho position (4f), however, moves the methyl chemical shift in the opposite (downfield) direction by an order of magnitude. The *p*-chloro analogue (4g) also induces a more downfield chemical shift of the methyl signal relative to that displayed by the parent compound 4a.

Computational Results. Are the extremely small changes observed in the chemical shift of the naphthyl methyl signal with varying substituents on the phenyl ring truly significant, or are they simply consequences of minor structural variations in the relative disposition of the methyl group and substituted phenyl ring in our series of compounds? While this question remains difficult to answer, the observed trends are nonetheless intriguing. It has been noted previously that a Hammett-type correlation, associating the chemical shifts of in-plane protons and substituents on the phenyl ring, could not be established.^{9c,16} Such a correlation also does not appear to exist for the

through-space shielding effects noted in our system (4a–j). One possible clue for the observed trend perhaps comes from the computational work of Martin's group, which modeled the through-space shielding effect of benzene–cation complexes on diatomic hydrogen (Figure 4).¹⁷ Martin and co-workers noted that complexation of the cation with one face of the benzene ring diminished the electron density on the opposite face of the ring, which is closer to H₂, resulting in a shielding of the proximal hydrogen. According to them, "...the magnitude of the shielding effect entirely due to complexation is substantial..." and "...the decreased π electron density on the side of the complexed benzene ring opposite the cation polarizes the covalent bond of diatomic hydrogen, increasing the electron density near the proximal hydrogen, with the consequence that the proximal hydrogen becomes more shielded."¹⁷ By analogy, it is conceivable that the electron density of the phenyl ring in our system is also perturbed in a similar fashion. Thus, as shown in Figure 5, one could envision an electron-withdrawing group diminishing the electron density of the phenyl ring and polarizing the C–H bonds of the naphthyl methyl ever so slightly that the hydrogens are now somewhat shielded (Figure 5a). An electron-donating group, on the other hand, would have just the opposite effect (Figure 5b). We do not, however, have a good explanation for the trend observed for the two para-substituted halogens. They could possibly represent a trade-off between their electron-withdrawing inductive effects and electron-donating mesomeric effects, with other, as yet unidentified, factors mixed in. Field effects (vide infra) could also play a role. In any event, the overall influence on the change in chemical shift of the probe methyl group caused by the substituents on the phenyl ring is quite small in most of the derivatives that we examined.

In recently published work, Rablen and Bally have described quantum chemical procedures for accurately computing chemical shifts of protons in organic molecules.¹⁸ Although the range of values for the methyl signal in our series, 4a–j, is extremely narrow, we decided to apply these new computational techniques¹⁸ to three exemplars in the series, namely 4a,

Table 1. Selected Crystallographic Data for 4b–e and 4g–i

entry	4b	4c	4d	4e	4g	4h	4i
chemical formula	C ₁₇ H ₁₃ NO ₂	C ₁₈ H ₁₄ O	C ₁₈ H ₁₃ N	C ₁₇ H ₁₃ F	C ₁₇ H ₁₃ Cl	C ₁₈ H ₁₆	C ₁₈ H ₁₆ O
crystal system	orthorhombic	monoclinic	monoclinic	monoclinic	monoclinic	monoclinic	orthorhombic
space group	<i>Pbca</i>	<i>C2/c</i>	<i>P2₁/c</i>	<i>P2₁/n</i>	<i>P2₁/c</i>	<i>P2₁/c</i>	<i>P2₁2₁2₁</i>
unit cell dimensions	a = 13.420 Å b = 7.671 Å c = 25.275 Å α = β = γ = 90°	a = 22.137 Å b = 7.901 Å c = 15.787 Å α = γ = 90° β = 104.31°	a = 11.380 Å b = 16.270 Å c = 7.267 Å α = γ = 90° β = 98.75°	a = 8.217 Å b = 9.041 Å c = 16.898 Å α = γ = 90° β = 94.55°	a = 16.582 Å b = 9.625 Å c = 17.605 Å α = γ = 90° β = 111.11°	a = 8.190 Å b = 24.346 Å c = 7.527 Å α = γ = 90° β = 117.11°	a = 8.223 Å b = 8.989 Å c = 17.940 Å α = β = γ = 90°
volume	2602.0 Å ³	2676 Å ³	1329.8 Å ³	1251.4 Å ³	2621.2 Å ³	1335.8 Å ³	1326.0 Å ³
Z	8	8	4	4	8	4	4
final R indices [<i>I</i> > 2σ(<i>I</i>)]	R1 = 0.0503 wR2 = 0.1101	R1 = 0.0674 wR2 = 0.1601	R1 = 0.0433 wR2 = 0.1123	R1 = 0.0508 wR2 = 0.1337	R1 = 0.0662 wR2 = 0.1856	R1 = 0.0489 wR2 = 0.1107	R1 = 0.0373 wR2 = 0.0831
final R indices (all data)	R = 0.0743 wR2 = 0.1209	R = 0.0736 wR2 = 0.1671	R = 0.0604 wR2 = 0.1254	R1 = 0.0728 wR2 = 0.1544	R1 = 0.0955 wR2 = 0.2135	R1 = 0.0791 wR2 = 0.1272	R1 = 0.0432 wR2 = 0.0858
interplanar angle between phenyl and naphthyl rings	85.59°	86.74°	74.91°	67.78°	76.51°	89.40°	69.08°
length of bond connecting phenyl and naphthyl rings	1.500 Å	1.503 Å	1.497 Å	1.492 Å	1.508 Å	1.500 Å	1.494 Å
distances between phenyl centroid and the two proximal protons of the 1-methyl group	2.851 Å	2.891 Å	3.052 Å	3.027 Å	2.985 Å	3.000 Å	3.007 Å
	3.191 Å	3.223 Å	3.070 Å	3.150 Å	3.182 Å	3.210 Å	3.193 Å

Table 2. Experimentally Obtained ¹H NMR Chemical Shift Data, in CDCl₃, for the Methyl Signal in 1-Methylnaphthalene and 4a–j^a

compound	δCH ₃ ppm	Δ(δCH ₃ for each compound – δCH ₃ for 4a), in ppm (Hz) ^b	Δ(δCH ₃ for each compound – δCH ₃ for 4a) in Hz/338 Hz ^c
1-methylnaphthalene	2.685	0.676 (338)	1
4a (X = H)	2.009	0 (0)	0
4b (X = <i>p</i> -NO ₂)	2.001	−0.008 (−4)	−0.012
4c (X = <i>p</i> -CHO)	2.006	−0.003 (−1.5)	−0.004
4d (X = <i>p</i> -CN)	1.990	−0.019 (−9.5)	−0.028
4e (X = <i>p</i> -F)	2.002	−0.007 (−3.5)	−0.010
4f (X = <i>o</i> -F)	2.084	0.075 (37.5)	0.111
4g (X = <i>p</i> -Cl)	2.026	0.017 (8.5)	0.025
4h (X = <i>p</i> -CH ₃) ^d	2.030	0.021 (10.5)	0.031
4i (X = <i>p</i> -OCH ₃)	2.037	0.028 (14)	0.041
4j (X = <i>p</i> -NH ₂)	2.085	0.076 (38)	0.112

^aThe shift of TMS (δ 0.000 ppm) is used as reference. ^bThis is the difference between each value in column 2 and the δCH₃ for 4a (2.009 ppm). ^cThis is ratio of each value in column 3 (in Hz) to 338 Hz. ^dThe reported data is for the methyl group on the naphthalene ring.

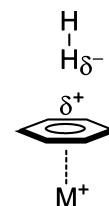
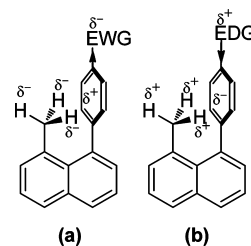
Figure 4. Polarization of diatomic hydrogen by a cation-π complex.¹⁷ This leads to a greater shielding of the hydrogen proximal to the ring.

Figure 5. Polarization of the methyl C–H bonds when an electron-withdrawing group (EWG) is present on the phenyl ring (a) as opposed to an electron-donating group (b).

4d, and 4j. Compound 4a (X = H) was chosen to serve as the standard, whereas 4d (X = CN) and 4j (X = NH₂) represented analogues with a strong electron-withdrawing and -donating group, respectively. Furthermore, according to our experimental observations, both 4d and 4j displayed the largest difference, in opposite directions, on the chemical shift of the methyl group, as compared to 4a.

The calculations were performed in two different ways. In one approach, structures of 4a, 4d, and 4j were optimized first at the B3LYP/6-31G* level of theory (Figure 6), and subsequently, the chemical shift of the methyl group was computed, in chloroform, on the optimized structures using GIAO/WP04/6-31G(d) and GIAO/WP04/cc-pVDZ procedures.¹⁸ In each case, the shifts for the three hydrogens in the methyl group were averaged and then scaled according to the recommended protocol.¹⁸

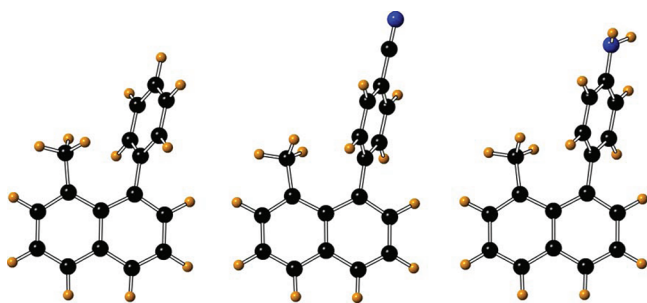


Figure 6. The B3LYP/6-31G* optimized structures of **4a** (left), **4d** (center), and **4j** (right).

In a second approach, benzene, benzonitrile, and aniline were optimized (B3LYP/6-31G*), and the naphthalene ring was then appended to each to generate “constrained” versions of **4a**, **4d**, and **4j**, with Cs symmetry, in which the two aryl rings were orthogonal to each other. Subsequently, the α and β angles were set to 124.339° and 124.997° , respectively, to splay the phenyl ring and the methyl group away from each other (Figure 7). These values represent the average of the

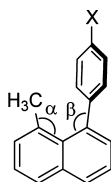


Figure 7. The α and β angles, averaged from the B3LYP/6-31G* optimized structures of **4a**, **4d**, and **4j**, worked out to 124.339° and 124.997° , respectively. These values were used to constrain the Cs structures shown in Figure 8.

corresponding angles in the optimized structures of **4a**, **4d**, and **4j** described above. Finally, the methyl group was oriented in two different ways, noted in parentheses as Me_1 and Me_2 for the structures shown in Figure 8. Note that $4j_{\text{pyr1}}$ and $4j_{\text{pyr2}}$

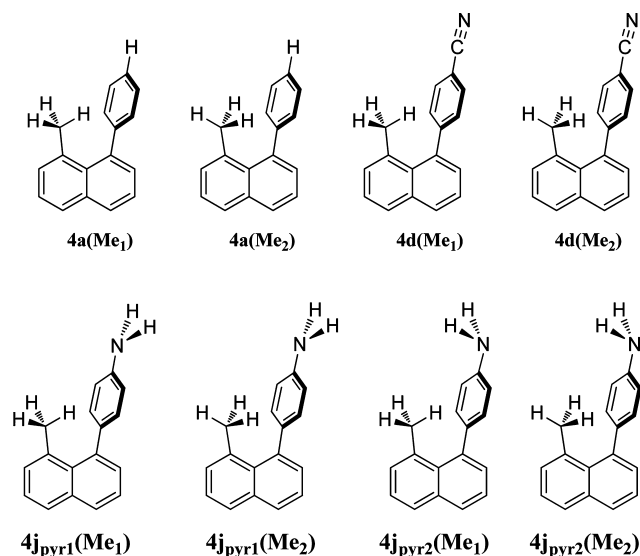


Figure 8. Constrained structures of **4a**, **4d**, and **4j** for ^1H NMR chemical shift calculations.

(Figure 8) represent conformations in which the amino group is pyramidalized in opposite directions. Thus, a total of six

hydrogen shifts (three for each orientation of the methyl group) for each set were computed, averaged, and scaled as before.¹⁹ These calculations also included chloroform as solvent, and the results are displayed in Table 3.

Table 3. Computed ^1H NMR Chemical Shift Data, in Chloroform, for the Methyl Signal in Optimized and Constrained Versions of **4a**, **4d**, and **4j**

compound	CH_3 shift in δ ppm GIAO/WP04/6-31G*	CH_3 shift in δ ppm GIAO/WP04/cc-pVDZ
4a optimized	1.968	2.050
4d optimized	1.954	2.031
4j optimized	2.078	2.152
4a (Me_1)/ 4a (Me_2) (constrained)	1.345	1.528
4d (Me_1)/ 4d (Me_2) (constrained)	1.291	1.471
$4j_{\text{pyr1}}$ (Me_1)/ $4j_{\text{pyr1}}$ (Me_2) (constrained)	1.540	1.724
$4j_{\text{pyr2}}$ (Me_1)/ $4j_{\text{pyr2}}$ (Me_2) (constrained)	1.455	1.730

As can be seen from Table 3, the computed methyl signals in the optimized structures of **4a**, **4d**, and **4j** more closely reproduce the experimental values and follow a trend that is consistent with that observed experimentally; i.e., the methyl group in the cyano derivative, **4d**, has a slightly more upfield shift than the one in the parent compound **4a**. By contrast, the methyl signal in the amino derivative, **4j**, is more downfield than the corresponding signal in **4a**. Furthermore, the amino group has a larger effect than the cyano substituent, just as observed in the experimental values. When the geometries of these compounds are artificially constrained so as to erase conformational differences among them with respect to the relative orientations of the phenyl ring and methyl group, all of the calculated values move further upfield. Even so, the computed and experimental methyl shifts display the same trend.

Another interesting experimental observation is the rather substantial change in the opposite direction (relative to **4a**) in going from **4e**, which has the fluorine para to the naphthyl ring, to **4f**, in which the fluorine is ortho. This suggests that another effect far more important than just electron density variations within the phenyl ring might be at play. Wheeler and Houk reported recently that, contrary to popular belief, electrostatic potentials above the centers of substituted benzenes are due primarily to through-space effects of substituents rather than the π polarization of the aryl ring.²⁰ Although counterintuitive, it has been calculated that local changes in electron density (“ π -electron-rich” vs “ π -electron-poor” aryl rings) are minor players in determining molecular electrostatic potentials, and field effects of the substituents are far more important.²¹ It is conceivable that an analogous situation perhaps exists for magnetic properties as well. In the optimized structure of **4e** (B3LYP/6-31G*), the methyl group (using its carbon as the reference point) is 5.589 \AA from the fluorine, which compares well with the distance of 5.506 \AA determined experimentally from the X-ray structure. In the calculated structure of **4f**, however, that distance drops to 3.306 \AA (Figure 9). As field effects are a function of distance, the greater proximity of the highly electronegative fluorine to the methyl group in **4f** compared to **4e** could account for the more pronounced effect on the methyl shift in the former.

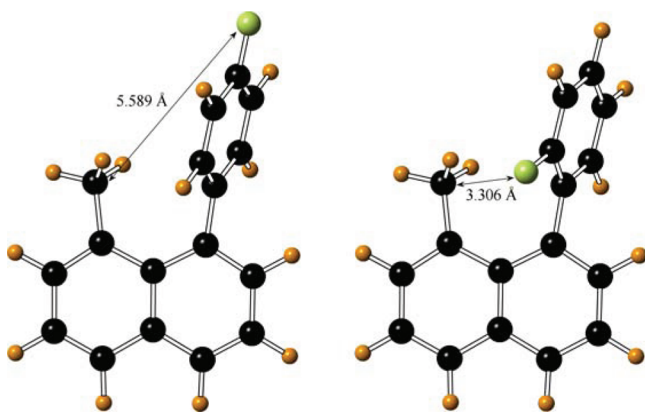


Figure 9. The B3LYP/6-31G* optimized structures of **4e** (left) and **4f** (right). The distance between the carbon of the methyl group and fluorine is noted in each structure.

These experimental findings are supported by chemical shift calculations, which were performed using the procedures described above, in chloroform as solvent, on the optimized structures of **4e** and **4f**. Using the average values of $\alpha = 124.393^\circ$ and $\beta = 125.394^\circ$, obtained from the optimized structures of **4e** and **4f**, constrained structures were built following the previously discussed method and are schematically shown in Figure 10. Calculations on these structures,

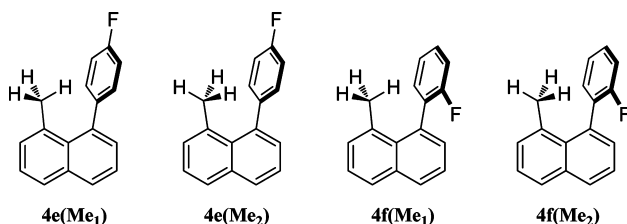


Figure 10. Constrained structures of **4a**, **4d**, and **4j** for ^1H NMR chemical shift calculations.

with chloroform as solvent, led to somewhat more upfield chemical shifts, but the experimentally observed trend was also reproduced by the computed values. The data are collected in Table 4.

Table 4. Computed ^1H NMR Chemical Shift Data, in Chloroform, for the Methyl Signal in Optimized and Constrained Versions of **4e** and **4f**

compound	CH ₃ shift in δ ppm GIAO/WP04/6-31G(d)	CH ₃ shift in δ ppm GIAO/WP04/cc-pVDZ
4e optimized	1.985	2.050
4f optimized	2.151	2.207
4e(Me₁)/4e(Me₂) (constrained)	1.362	1.531
4f(Me₁)/4f(Me₂) (constrained)	1.424	1.578

Conclusions. In our particular system, namely compounds **4a–j**, it is clear that the substituents on the phenyl ring have very little influence on the chemical shift of the methyl protons that are in its (phenyl ring's) shielding zone. This is in sharp contrast to the profound effect that phenyl substituents are known to have on the chemical shifts of protons that are on the periphery of the ring. Within the small effects that were

observed for the signal of the naphthyl methyl in **4a–j**, it appears that electron-withdrawing groups have a slightly shielding effect, whereas electron donors are somewhat deshielding. These small effects are rationalized in terms of through-space polarization of the C–H bonds of the methyl group by the phenyl ring. Field effects, which are dependent on the proximity of the substituent to the methyl group, appear to be especially important as exemplified by the fluoro derivatives **4e** and **4f**. Chemical shift calculations on optimized structures of selected molecules in the series are consistent with the experimental observations. Even when these molecules were constrained to remove conformational differences among them with respect to the relative orientations of the phenyl ring and methyl group, the trends in the computed chemical shifts parallel those found experimentally.

EXPERIMENTAL METHODS

General Experimental Procedures. All solvents and reagents were used as obtained from commercial sources. Unless otherwise noted, all reactions were carried out under an argon atmosphere in oven-dried glassware. The synthesis of 1-bromo-8-methylnaphthalene (**6**) was carried out following literature procedures.¹³ Microwave reactions were carried out in a scientific reactor equipped with a single magnetron capable of up to 1200 W of power output. Flash chromatography was performed on prepacked silica gel columns (70–230 mesh). NMR spectra were recorded at 500 MHz for ^1H and 125 MHz for ^{13}C in CDCl_3 . The shifts are reported in δ ppm and referenced to either tetramethylsilane (TMS) (for ^1H NMR spectra) or the central peak of the carbon triplet signal of CDCl_3 (for ^{13}C NMR spectra). FTIR spectra were acquired with an attenuated total reflectance (ATR) accessory for solids, and in the neat form, with sodium chloride plates, for liquids. GC–MS data were obtained with a capillary gas chromatograph interfaced with a quadrupole, triple-axis mass selective detector operating in the electron impact (EI) mode. High resolution mass spectra were obtained on a direct analysis in real time–time-of-flight (DART-TOF) mass spectrometer. Melting points are uncorrected.

General Procedure for the Suzuki–Miyaura Coupling of **6 with Aryl Boronic Acids.**¹⁴ **Preparation of Compounds **4a–i**.** To a mixture of the appropriate arylboronic acid (1.5 mmol), **6** (1 mmol), cesium carbonate (1 mmol), and anhydrous DMF (10 mL), degassed with nitrogen or argon, was added tetrakis(triphenylphosphine)palladium(0) (0.05 mmol). The mixture was stirred magnetically and heated by microwave irradiation at 140°C for 45 min, allowed to cool to room temperature, and reheated at 140°C for another 45 min. The reaction mixture was then cooled to room temperature again, diluted with ethyl acetate and water, and filtered through a pad of Celite under vacuum. The organic and aqueous layers were separated, and the latter was extracted with additional ethyl acetate. The organic layers were combined, washed with water and brine, dried over anhydrous MgSO_4 , gravity filtered, and freed of solvent. The crude material was adsorbed onto silica gel and purified using flash chromatography (either hexanes or 5% ethyl acetate in hexanes). Yields and characterization data for each compound are reported below.

1-Methyl-8-phenylnaphthalene (4a**).**²² Clear, colorless, viscous liquid: yield 17%; ^1H NMR δ 7.85 (dd, $J = 8.2, 1.4$ Hz, 1H), 7.77 (d, $J = 8.1$ Hz, 1H), 7.43 (dd, $J = 8.1, 7.0$ Hz, 1H), 7.39–7.32 (m, 6H), 7.30 (dd, $J = 7.0, 1.4$ Hz, 1H), 7.22 (d, $J = 7.0$ Hz, 1H), 2.01 (s, 3H); ^{13}C NMR δ 145.3, 140.6, 135.6, 135.2, 131.2, 129.9, 129.8, 129.7, 129.0, 127.7, 127.6, 126.9, 125.7, 124.5, 25.3; FTIR (neat) ν 3055, 1582, 1492, 1444, 1030, 1039, 820, 773, 703 cm^{-1} ; LRMS (EI) m/z 218 (M^+), 203, 189, 101.

1-Methyl-8-(4-nitrophenyl)naphthalene (4b**).** Bright yellow, crystalline solid: yield 62%; mp $157\text{--}160^\circ\text{C}$; ^1H NMR δ 8.27 (d, $J = 8.4$ Hz, 2H), 7.91 (dd, $J = 8.2, 1.3$ Hz, 1H), 7.81 (d, $J = 8.1$ Hz, 1H), 7.52 (d, $J = 8.4$ Hz, 2H), 7.47 (dd, $J = 8.1, 7.1$ Hz, 1H), 7.44–7.40 (m, 1H), 7.30–7.25 (m, 2H), 2.00 (s, 3H); ^{13}C NMR δ 152.3, 147.1, 138.1, 135.2, 134.6, 130.60, 130.55, 130.5, 130.2, 129.6, 127.8, 126.2,

124.4, 123.1, 25.7; FTIR (ATR) ν 2985, 1594, 1515, 1345, 1276, 1260, 851, 822, 751 cm^{-1} ; LRMS (EI) m/z 263 (M^+), 215, 202, 189.

4-(8-Methylnaphthalen-1-yl)benzaldehyde (4c). Pale yellow, crystalline solid: yield 84%; mp 79–82 °C; ^1H NMR δ 10.10 (s, 1H), 7.92 (d, $J = 8.2$ Hz, 2H), 7.90 (dd, $J = 8.2, 1.3$ Hz, 1H), 7.80 (d, $J = 8.1$ Hz, 1H), 7.53 (d, $J = 8.1$ Hz, 2H), 7.46 (dd, $J = 8.1, 7.0$ Hz, 1H), 7.42–7.38 (m, 1H), 7.30–7.25 (m, 2H), 2.00 (s, 3H); ^{13}C NMR δ 192.2, 151.9, 139.1, 135.20, 135.18, 135.0, 130.7, 130.5, 130.3, 129.8, 129.6, 129.3, 127.7, 126.0, 124.5, 25.5; FTIR (ATR) ν 2933, 2716, 1699, 1600, 1207, 1167, 821, 777, 761 cm^{-1} ; LRMS (EI) m/z 246 (M^+), 215, 202, 189.

4-(8-Methylnaphthalen-1-yl)benzotrile (4d). Colorless, crystalline solid: yield 53%; mp 139–143 °C; ^1H NMR δ 7.92–7.89 (m, 1H), 7.82–7.78 (m, 1H), 7.70 (dd, $J = 7.9, 0.6$ Hz, 2H), 7.47 (dd, $J = 7.9, 0.6$ Hz, 2H), 7.46–7.44 (m, 1H), 7.41 (dd, $J = 8.1, 7.1$ Hz, 1H), 7.28–7.26 (m, 1H), 7.25 (dd, $J = 6.4, 0.9$ Hz, 1H), 1.99 (s, 3H). ^{13}C NMR δ 150.3, 138.5, 135.2, 134.7, 131.61, 130.62, 130.5, 130.4, 130.0, 129.6, 127.8, 126.1, 124.5, 119.2, 111.0, 25.6; FTIR (ATR) ν 2967, 2224, 1605, 1454, 1367, 840, 850, 822, 774 cm^{-1} ; LRMS (EI) m/z 243 (M^+), 228, 215, 202, 189.

1-(4-Fluorophenyl)-8-methylnaphthalene (4e). Colorless solid: yield 55%; mp 58–61 °C; ^1H NMR δ 7.84 (dd, $J = 8.2, 1.4$ Hz, 1H), 7.76 (d, $J = 8.1$ Hz, 1H), 7.41 (dd, $J = 8.1, 7.0$ Hz, 1H), 7.35 (dd, $J = 8.1, 7.1$ Hz, 1H), 7.30–7.24 (m, 3H), 7.23–7.20 (m, 1H), 7.06 (t, $J = 8.8$ Hz, 2H), 2.00 (s, 3H); ^{13}C NMR δ 162.2 (d, $J = 245.5$ Hz), 141.2 (d, $J = 3.5$ Hz), 139.4, 135.3 (d, $J = 20.2$ Hz), 131.24, 131.20, 131.14, 130.07, 129.9 (d, $J = 1.0$ Hz), 129.3, 127.7, 125.8, 124.5, 114.58 (d, $J = 21.3$ Hz), 25.4; FTIR (ATR) ν 3040, 2971, 1602, 1511, 1494, 1212, 1157, 842, 817, 757, 726 cm^{-1} ; LRMS (EI) m/z 236 (M^+), 220, 215, 202, 189.

1-(2-Fluorophenyl)-8-methylnaphthalene (4f). Clear, colorless, viscous liquid: yield 13%; ^1H NMR δ 7.89 (dd, $J = 8.2, 1.4$ Hz, 1H), 7.80–7.76 (m, 1H), 7.46 (dd, $J = 8.2, 7.0$ Hz, 1H), 7.41–7.29 (m, 4H), 7.25–7.22 (m, 1H), 7.18 (td, $J = 7.5, 1.2$ Hz, 1H), 7.12 (ddd, $J = 9.4, 8.3, 1.1$ Hz, 1H), 2.08 (s, 3H); ^{13}C NMR δ 160.2 (d, $J = 244.0$ Hz), 135.1 (d, $J = 11.2$ Hz), 133.5, 132.9, 132.7, 132.1 (d, $J = 3.2$ Hz), 131.6, 130.1 (d, $J = 0.7$ Hz), 129.95, 129.88, 129.3 (d, $J = 7.8$ Hz), 127.9, 125.7, 124.6, 123.7 (d, $J = 3.6$ Hz), 115.4 (d, $J = 22.2$ Hz), 23.9; FTIR (neat) ν 3057, 2969, 1580, 1492, 1448, 1215, 1106, 816, 773, 758 cm^{-1} ; LRMS (EI) m/z 236 (M^+), 215, 220, 202, 189; HRMS (DART-TOF) calcd for $\text{C}_{17}\text{H}_{14}\text{F}$ [$M + \text{H}$] $^+$ 237.1080, found 237.1067.

1-(4-Chlorophenyl)-8-methylnaphthalene (4g). Colorless, crystalline solid: yield 31%; mp 73–78 °C; ^1H NMR δ 7.85 (dd, $J = 8.2, 1.2$ Hz, 1H), 7.77 (d, $J = 8.1$ Hz, 1H), 7.47–7.38 (m, 2H), 7.36 (d, $J = 8.3$ Hz, 2H), 7.28–7.22 (m, 4H), 2.03 (s, 3H); ^{13}C NMR δ 143.6, 139.2, 135.3, 135.2, 133.0, 131.05, 131.04, 130.1, 129.8, 129.4, 127.9, 127.7, 125.8, 124.5, 25.5; FTIR (ATR) ν 3035, 2968, 1595, 1485, 1088, 1013, 831, 817, 769 cm^{-1} ; LRMS (EI) m/z 252 (M^+), 237, 215, 202, 189, 152, 107.

1-Methyl-8-(p-tolyl)naphthalene (4h). Colorless, crystalline solid: yield 39%; mp 64–67 °C; ^1H NMR δ 7.83 (dd, $J = 8.2, 1.4$ Hz, 1H), 7.77–7.74 (m, 1H), 7.42 (dd, $J = 8.1, 7.0$ Hz, 1H), 7.35 (dd, $J = 8.1, 7.0$ Hz, 1H), 7.29 (dd, $J = 7.0, 1.5$ Hz, 1H), 7.22 (dd, $J = 6.0, 2.2$ Hz, 3H), 7.19 (d, $J = 7.8$ Hz, 2H), 2.43 (s, 3H), 2.03 (s, 3H); ^{13}C NMR δ 142.4, 140.6, 136.5, 135.7, 135.2, 131.3, 129.8, 129.8, 129.7, 128.9, 128.4, 127.6, 125.6, 124.5, 25.3, 21.5; FTIR (ATR) ν 2960, 1514, 1500, 1442, 1107, 1036, 1023, 819, 775 cm^{-1} ; LRMS (EI) m/z 232 (M^+), 217, 215, 202, 189, 165, 101.

1-(4-Methoxyphenyl)-8-methylnaphthalene (4i). Colorless, crystalline solid: yield 50%; mp 91–95 °C; ^1H NMR δ 7.82 (dd, $J = 8.1, 1.4$ Hz, 1H), 7.75 (d, $J = 8.1$ Hz, 1H), 7.41 (dd, $J = 8.1, 7.0$ Hz, 1H), 7.35 (dd, $J = 8.1, 7.1$ Hz, 1H), 7.29 (dd, $J = 7.0, 1.4$ Hz, 1H), 7.25–7.20 (m, 3H), 6.92 (d, $J = 8.7$ Hz, 2H), 3.86 (s, 3H), 2.04 (s, 3H); ^{13}C NMR δ 158.8, 140.3, 137.7, 135.7, 135.2, 131.5, 130.7, 129.9, 129.9, 128.9, 127.6, 125.6, 124.5, 113.1, 55.5, 25.3; FTIR (ATR) ν 2955, 2928, 1606, 1515, 1490, 1438, 1239, 1183, 1174, 1033, 835, 819, 777 cm^{-1} ; LRMS (EI) m/z 248 (M^+), 233, 215, 202, 189.

Synthesis of 4-(8-Methylnaphthalen-1-yl)aniline (4j). A solution of **7b** (100 mg, 0.38 mmol) in ethyl acetate (10 mL) was degassed by bubbling with Ar. About 15 mg Pd/C was then added,

and the reaction mixture was magnetically stirred under an atmosphere of hydrogen for 5 h. The reaction mixture was diluted with additional ethyl acetate and filtered under vacuum through a Celite pad. The filtrate was extracted with 6 M HCl, and the resulting aqueous layer was made basic using 50% aqueous NaOH. The solution was extracted with ethyl acetate. Removal of solvent afforded the product as a liquid in 80% yield: ^1H NMR δ 7.80 (dd, $J = 8.1, 1.4$ Hz, 1H), 7.76–7.72 (m, 1H), 7.40 (dd, $J = 8.1, 7.0$ Hz, 1H), 7.34 (dd, $J = 8.1, 7.0$ Hz, 1H), 7.29 (dd, $J = 7.0, 1.5$ Hz, 1H), 7.22–7.19 (m, 1H), 7.10 (d, $J = 8.5$ Hz, 2H), 6.70 (d, $J = 8.5$ Hz, 2H), 3.97–3.16 (br, 2H), 2.08 (s, 3H); ^{13}C NMR δ 145.4, 140.8, 135.9, 135.7, 135.3, 131.7, 130.6, 129.9, 129.7, 128.6, 127.5, 125.5, 124.5, 114.5, 25.3. FTIR (ATR) ν 3456, 3374, 2964, 1621, 1516, 1454, 1263, 1179, 1098, 1038, 1033, 819, 774 cm^{-1} ; LRMS (EI) m/z 233 (M^+), 215, 202, 189; HRMS (DART-TOF) calcd for $\text{C}_{17}\text{H}_{16}\text{N}$ [$M + \text{H}$] $^+$ 234.1283, found 234.1283.

General Procedure for X-ray Structure Determination. X-ray data were collected at 173 K for **4b**, **4c**, **4e**, and **4g–i**, and 110 K for **4d**, on a Bruker Smart Apex CCD diffractometer using graphite monochromated Mo $K\alpha$ radiation ($\lambda = 0.71073$ Å). Except for **4c**, which exhibited a positional disorder in the aldehyde functionality and was processed separately (see the Supporting Information for details), all data were processed with the Bruker Apex2 suite of programs.²³ The frames were integrated with the Bruker SAINT software package using a narrow-frame algorithm, and data were corrected for absorption effects using the multiscan method (SADABS).²⁴ The structures were solved by direct methods and refined by full-matrix least-squares on F^2 , using the Bruker SHELXTL software package.^{19,25} All nonhydrogen atoms were refined anisotropically, and the hydrogens were calculated on a riding model. The software program enCIFer²⁶ was used in conjunction with the checkCIF/Platon facility of IUCr to validate cif files.

Computational Methods. Geometries of compounds **4a**, **4d**, **4e**, **4f**, and **4j** were fully optimized with the Gaussian 09²⁷ suite of programs with the hybrid Hartree–Fock density functional theory method (B3LYP)²⁸ and 6-31G* basis set. Vibrational frequency calculations, carried out at the same level of theory, allowed the characterization of the located stationary points as minima (no imaginary frequencies). The WP04²⁹ functional may be invoked in Gaussian 09 by entering the BLYP keyword and adding internal options as follows: iop (3/76=1000001189,3/77=0961409999,3/78=0000109999).^{18a} The GIAO/WP04/6-31G(d) chemical shift was scaled in accord with the following formula: scaled shift $\delta = (32.433 - \text{calculated isotropic magnetic shielding})/0.9927$.^{18a} For GIAO/WP04/cc-pVDZ calculations, the scaled chemical shift $\delta = (31.844 - \text{calculated isotropic magnetic shielding})/1.0205$.^{18b}

■ ASSOCIATED CONTENT

● Supporting Information

Copies of ^1H and ^{13}C NMR spectra, FTIR spectra, and GC–MS data for compounds **4a–j**. Cartesian coordinates and energies for the B3LYP/6-31G(d) optimized structures of **4a**, **4d**, **4e**, **4f**, and **4j**. Computed isotropic magnetic shielding values and chemical shifts. Notes about the X-ray structure determination for compound **4c**. Crystallographic information files (CIFs) for compounds **4b–e** and **4g–i**. This material is available free of charge via the Internet at <http://pubs.acs.org>.

■ AUTHOR INFORMATION

Corresponding Author

*E-mail: dmthamat@colby.edu.

Present Address

[†]Department of Chemistry, University of Wisconsin-Madison, 1101 University Avenue, Madison, Wisconsin 53706, United States.

Notes

The authors declare no competing financial interest.

ACKNOWLEDGMENTS

We gratefully acknowledge support of this work by the National Science Foundation through Grant No. CHE-1012914, and a grant from the SD Bechtel, Jr. Foundation to C.W.A. We thank Professors Ned H. Martin, Paul von Ragué Schleyer, and Hans Reich for helpful discussions, and Professor Paul Rablen for providing valuable guidance for the computation of chemical shifts. We are indebted to Professor Bruce Foxman for assistance with the X-ray structure solution of **4c** and Dr. Carlton Rauschenberg for the DART-TOF high resolution mass spectral data.

REFERENCES

- (1) Pauling, L. *J. Chem. Phys.* **1936**, *4*, 673.
- (2) Lonsdale, K. *Proc. R. Soc. London, Ser. A* **1937**, *159*, 149.
- (3) (a) London, F. *J. Phys. Radium* **1937**, *8*, 397. (b) London, F. *J. Chem. Phys.* **1937**, *5*, 837.
- (4) (a) Pople, J. A. *J. Chem. Phys.* **1956**, *24*, 1111. (b) Bernstein, H. J.; Schneider, W. G.; Pople, J. A. *Proc. R. Soc. London, Ser. A* **1956**, *236*, 515. (c) Pople, J. A. *Mol. Phys.* **1958**, *1*, 175.
- (5) (a) Heine, T.; Corminboeuf, C.; Seifert, G. *Chem. Rev.* **2005**, *105*, 3889. (b) Lazzeretti, P. *Phys. Chem. Chem. Phys.* **2004**, *6*, 217. (c) Mitchell, R. H. *Chem. Rev.* **2001**, *101*, 1301. (d) Gomes, J. A.; Mallion, R. B. *Chem. Rev.* **2001**, *101*, 1349. (e) Lazzeretti, P. *Prog. Nucl. Magn. Reson. Spectrosc.* **2000**, *36*, 1. (f) Schleyer, P. v. R.; Jiao, H. *Pure Appl. Chem.* **1996**, *68*, 209. (g) Haigh, C. W.; Mallion, R. B. In *Progress in Nuclear Magnetic Resonance Spectroscopy*; Emsley, J. W., Feeney, J., Sutcliffe, L. H., Eds.; Pergamon Press: Oxford, 1979; Vol. 13, p 303.
- (6) (a) Wannere, C. S.; Schleyer, P. v. R. *Org. Lett.* **2003**, *5*, 605. (b) Fleischer, U.; Kutzelnigg, W.; Lazzeretti, P.; Muehlenkamp, V. *J. Am. Chem. Soc.* **1994**, *116*, 5298. (c) Blustin, P. H. *Mol. Phys.* **1980**, *39*, 565. (d) Blustin, P. H. *Chem. Phys. Lett.* **1979**, *64*, 507. (e) Blustin, P. H. *Mol. Phys.* **1978**, *36*, 1441. (f) Musher, J. I. *J. Chem. Phys.* **1967**, *46*, 1219. (g) Musher, J. I. *Adv. Magn. Reson.* **1966**, *2*, 177. (h) Musher, J. I. *J. Chem. Phys.* **1965**, *43*, 4081.
- (7) (a) Viglione, R. G.; Zanasi, R.; Lazzeretti, P. *Org. Lett.* **2004**, *6*, 2265. (b) Gaidis, J. M.; West, R. *J. Chem. Phys.* **1967**, *46*, 1218.
- (8) Faglioni, F.; Ligabue, A.; Pelloni, S.; Soncini, A.; Viglione, R. G.; Ferraro, M. B.; Zanasi, R.; Lazzeretti, P. *Org. Lett.* **2005**, *7*, 3457.
- (9) (a) Silverstein, R. M.; Webster, F. X.; Kiemle, D. J. *Spectrometric Identification of Organic Compounds*, 7th ed.; John Wiley & Sons: Hoboken, NJ, 2005. (b) Günther, H. *NMR Spectroscopy: Basic Principles, Concepts, And Applications in Chemistry*, 2nd ed.; Wiley: Chichester, U. K., 1995. (c) Batts, B. D.; Pallos, G. *Org. Magn. Reson.* **1980**, *13*, 349. (d) Lazzeretti, P.; Taddei, F. *Org. Magn. Reson.* **1971**, *3*, 283. (e) Schug, J. C. *J. Chem. Phys.* **1967**, *46*, 2447.
- (10) SDBSWeb; National Institute of Advanced Industrial Science and Technology. <http://riodb01.ibase.aist.go.jp/sdbs/> (accessed January 30, 2011).
- (11) Martin, N. H.; Allen, N. W.; Moore, J. C. *J. Mol. Graphics Modell.* **2000**, *18*, 242.
- (12) Penn, L.; Mallory, F. B. *J. Magn. Reson.* **1975**, *18*, 6.
- (13) Kesharwani, T.; Larock, R. C. *Tetrahedron* **2008**, *64*, 6090.
- (14) (a) Alonso, F.; Beletskaya, I. P.; Yus, M. *Tetrahedron* **2008**, *64*, 3047. (b) Suzuki, A.; Brown, H. C. *Organic Synthesis via Boranes*; Aldrich: Milwaukee, WI, 2003; Vol. 3. (c) Miyaura, N. *Top. Curr. Chem.* **2002**, *219*, 11. (d) Miyaura, N.; Suzuki, A. *Chem. Rev.* **1995**, *95*, 2457.
- (15) Pieters, G.; Terrasson, V.; Gaucher, A.; Prim, D.; Marrot, J. *Eur. J. Org. Chem.* **2010**, *2010*, 5800.
- (16) Tribble, M. T.; Traynham, J. G. In *Advances in Linear Free Energy Relationships*; Chapman, N. B., Shorter, J., Eds.; Plenum: London, 1972; p 143.
- (17) Martin, N. H.; Main, K. L.; Pyles, A. K. *J. Mol. Graphics Modell.* **2007**, *25*, 806.
- (18) (a) Jain, R.; Bally, T.; Rablen, P. R. *J. Org. Chem.* **2009**, *74*, 4017. (b) Bally, T.; Rablen, P. R. *J. Org. Chem.* **2011**, *76*, 4818.
- (19) For an analogous procedure for averaging methyl chemical shifts, see: Martin, N. H.; Allen, N. W. III; Minga, E. K.; Ingrassia, S. T.; Brown, J. D. *J. Am. Chem. Soc.* **1998**, *120*, 11510.
- (20) Wheeler, S. E.; Houk, K. N. *J. Am. Chem. Soc.* **2009**, *131*, 3126.
- (21) Wheeler, S. E.; Houk, K. N. *J. Chem. Theory Comput.* **2009**, *5*, 2301.
- (22) Mallory, F. B.; Mallory, C. W. *Org. React. (Hoboken, NJ, U. S.)* **1984**, *30*, 1.
- (23) APEX2; Bruker AXS Inc.: Madison, WI, 2009.
- (24) Sheldrick, G. M. *SADABS*; University of Gottingen: Gottingen, Germany, 2008.
- (25) Sheldrick, G. M. *Acta Crystallogr.* **2008**, *A64*, 112.
- (26) Allen, F. H.; Johnson, O.; Shields, G. P.; Smith, B. R.; Towler, M. *J. Appl. Crystallogr.* **2004**, *37*, 335.
- (27) Frisch, M. J.; Trucks, G. W.; Schlegel, H. B.; Scuseria, G. E.; Robb, M. A.; Cheeseman, J. R.; Scalmani, G.; Barone, V.; Mennucci, B.; Petersson, G. A.; Nakatsuji, H.; Caricato, M.; Li, X.; Hratchian, H. P.; Izmaylov, A. F.; Bloino, J.; Zheng, G.; Sonnenberg, J. L.; Hada, M.; Ehara, M.; Toyota, K.; Fukuda, R.; Hasegawa, J.; Ishida, M.; Nakajima, T.; Honda, Y.; Kitao, O.; Nakai, H.; Vreven, T.; Montgomery, J. A., Jr.; Peralta, J. E.; Ogliaro, F.; Bearpark, M.; Heyd, J. J.; Brothers, E.; Kudin, K. N.; Staroverov, V. N.; Kobayashi, R.; Normand, J.; Raghavachari, K.; Rendell, A.; Burant, J. C.; Iyengar, S. S.; Tomasi, J.; Cossi, M.; Rega, N.; Millam, J. M.; Klene, M.; Knox, J. E.; Cross, J. B.; Bakken, V.; Adamo, C.; Jaramillo, J.; Gomperts, R.; Stratmann, R. E.; Yazyev, O.; Austin, A. J.; Cammi, R.; Pomelli, C.; Ochterski, J. W.; Martin, R. L.; Morokuma, K.; Zakrzewski, V. G.; Voth, G. A.; Salvador, P.; Dannenberg, J. J.; Dapprich, S.; Daniels, A. D.; Farkas, O.; Foresman, J. B.; Ortiz, J. V.; Cioslowski, J.; Fox, D. J. *Gaussian 09, Revision A.02*; Gaussian, Inc.: Wallingford, CT, 2009.
- (28) (a) Becke, A. D. *Phys. Rev. A: At., Mol., Opt. Phys.* **1988**, *38*, 3098. (b) Lee, C.; Yang, W.; Parr, R. G. *Phys. Rev. B: Condens. Matter Mater. Phys.* **1988**, *37*, 785. (c) Becke, A. D. *J. Chem. Phys.* **1993**, *98*, 5648.
- (29) Wiitala, K. W.; Hoye, T. R.; Cramer, C. J. *J. Chem. Theory Comput.* **2006**, *2*, 1085.